OsteoArthritis and Cartilage (2006) **14,** 1265–1271

doi:10.1016/j.joca.2006.06.002

Osteoarthritis and Cartilage

International Cartilage Repair Society

OARSI OSTEOARTHRITIS RESEARCH SOCIETY INTERNATIONAL

T_2 relaxation time mapping reveals age- and species-related diversity of collagen network architecture in articular cartilage

M. J. Nissi B.Sc.†*, J. Rieppo BM‡, J. Töyräs Ph.D.§, M. S. Laasanen Ph.D.‖, I. Kiviranta Ph.D.¶, J. S. Jurvelin Ph.D.†‖ and M. T. Nieminen Ph.D.#

† *Department of Physics, University of Kuopio, Kuopio, Finland*

‡ *Department of Anatomy, University of Kuopio, Kuopio, Finland*

§ *Department of Clinical Neurophysiology, Kuopio University Hospital and University of Kuopio, Finland*

‖ *Department of Clinical Physiology and Nuclear Medicine, Kuopio University Hospital, Kuopio, Finland*

¶ *Department of Orthopaedics and Traumatology, Jyväskylä Central Hospital, Jyväskylä, Finland*

Department of Diagnostic Radiology, Oulu University Hospital, Oulu, Finland

Summary

Objective: The magnetic resonance imaging (MRI) parameter T_2 relaxation time has been shown to be sensitive to the collagen network architecture of articular cartilage. The aim of the study was to investigate the agreement of T_2 relaxation time mapping and polarized light microscopy (PLM) for the determination of histological properties (i.e., zone and fibril organization) of articular cartilage.

Methods: T_2 relaxation time was determined at 9.4 T field strength in healthy adult human, juvenile bovine and juvenile porcine patellar cartilage, and related to collagen anisotropy and fibril angle as measured by quantitative PLM.

Results: Both T_2 and PLM revealed a mutually consistent but varying number of collagen-associated laminae (3, 3–5 or 3–7 laminae in human, porcine and bovine cartilage, respectively). Up to 44% of the depth-wise variation in T_2 was accounted for by the changing anisotropy of collagen fibrils, confirming that T_2 contrast of articular cartilage is strongly affected by the collagen fibril anisotropy. A good correspondence was observed between the thickness of T_2-laminae and collagenous zones as determined from PLM anisotropy measurements ($r = 0.91$, $r = 0.95$ and $r = 0.91$ for human, bovine and porcine specimens, respectively).

Conclusions: According to the present results, T_2 mapping is capable of detecting histological differences in cartilage collagen architecture among species, likely to be strongly related to the differences in maturation of the tissue. This diversity in the MRI appearance of healthy articular cartilage should also be recognized when using juvenile animal tissue as a model for mature human cartilage in experimental studies.

Key words: Articular cartilage, T_2 relaxation, Polarized light microscopy, Collagen, Anisotropy, Fibril angle.

Introduction

Articular cartilage is a tissue mainly composed of collagen, proteoglycans (PGs) and interstitial water. All constituents, and their complex interactions, have an essential role in the mechanical properties of cartilage[1]. Degradation of the macromolecular constituents critically affects the mechanical integrity of the tissue[2]. The damage of the collagen fibril network is particularly deleterious to cartilage, since the resilience and tensile properties of cartilage are widely maintained by the collagen network and its disruption is understood to be irreversible[1]. Therefore, it is critical to understand the structural diversity and organization of the collagen network of healthy cartilage tissue when pursuing, for example, cartilage diagnostics or the assessment of repair healing.

T_2 relaxation time of articular cartilage is sensitive to the three-dimensional (3-D) arrangement of the collagen fibrils[3–6], collagen concentration[6–8] and the water content of tissue[6,9,10] while contradicting results have been published on its sensitivity for PG content[6,11,12]. Dipolar coupling of collagen-associated water provides a significant source of T_2 relaxation in articular cartilage. The strength of this interaction is orientation-dependent and reaches its minimum at an angle of 54.7° between the static field and the axis of interacting protons, the so-called "magic angle". Consequently, T_2 changes along cartilage thickness are reported to follow the orientational changes in the collagen fibril network[3,4,13]. Using appropriate arrangement of the articular surface with respect to the $\mathbf{B}_0$ field the resulting laminated appearance in T_2 maps or T_2-weighted images approximately corresponds to the histological collagenous zones: the superficial zone (I, orientation of collagen fibrils parallel to the articular surface), the transitional zone (II, random fibril orientation) and the deep or radial zone (III, fibrils perpendicular to the articular surface and perpendicular to the bone)[4,a]. More than three magnetic resonance imaging (MRI) laminae have previously been reported in

*Address correspondence and reprint requests to: Mikko Johannes Nissi, B.Sc., Department of Physics, University of Kuopio, POB 1627, Savilahdentie 9, 70211 Kuopio, Finland. Tel: 358-17-162341; Fax: 358-17-162585; E-mail: nissi@venda.uku.fi, http://www.luotain.uku.fi

Received 17 November 2005; revision accepted 5 June 2006.

[a]In this study, the term "zone" is used when referring to histological tissue layers, while "lamina" refers to tissue layers observed in MRI.

young bovine patellar cartilage[3,11], humeral or femoral condyles of juvenile porcine cartilage[5,14] and in the peripheral area of the humeral head of young canines[15]. These laminae are observed as additional zones in polarized light microscopy (PLM) of the collagen network[4,5,14–17]. Recently, the novel PLM method developed in our group provides a true measure of anisotropy, i.e., parallelism of collagen fibrils[18]. The complex laminar appearance, anticipated to relate to orientational changes in the collagen fibrils, has been related to tissue immaturity[3] and structural differences arising from varying load-bearing conditions within the joint and between species[14,15].

The aims of the present study were to (1) investigate whether T_2 mapping can reproduce histologically detectable variations in the arrangement of the collagen network of healthy mature and immature articular cartilage, as well as to verify the agreement of laminae by T_2 and PLM measurements, and (2) evaluate the effect of collagen orientation and organization on the depth-wise variation of T_2 relaxation time. This was accomplished by measuring cartilage T_2 relaxation times from different sources, i.e., from healthy mature human, juvenile bovine and juvenile porcine patellar cartilage at 9.4 T, and relating the T_2 findings to the collagen anisotropy and the fibril angle as determined by modern quantitative PLM techniques[18].

Methods

SAMPLE PREPARATION

Non-arthritic human cadaver knee joints ($n = 12$, age = 20–78 years) were obtained within 48 h *post mortem* from the Jyväskylä Central Hospital, Jyväskylä, Finland with the permission from the national authority (National Authority for Medicolegal Affairs, Helsinki, Finland, permission 1781/32/200/01). Intact bovine ($n = 12$, age = 1–3 years) and porcine knee joints ($n = 11$, age about 4 months) were obtained from the local abattoir (Atria Oyj, Kuopio, Finland). For all samples, an osteochondral plug (diameter = 16 mm) was harvested from the same anatomical location, lateroproximal patella, immersed in phosphate buffered saline (PBS) containing enzyme inhibitors (5 mM ethylenediaminetetraacetic acid (EDTA) (Riedel-de-Haen, Seelze, Germany) and 5 mM benzamide HCl (Sigma Chemical Co., St. Louis, MO, USA)), and was frozen at −20 °C (Fig. 1) For MRI measurements, a 4-mm full-thickness cartilage disk without subchondral bone was detached from each block and the adjacent tissue from the osteochondral core was used for microscopical evaluation (Fig. 1). All samples passed two freeze-thaw cycles before MRI measurements.

MRI MEASUREMENTS

The samples were sealed in a test tube (dia. = 5 mm) filled with PBS. The test tube was then positioned into a high resolution spectroscopy coil (dia. = 5 mm, coil length ~ 12 mm Varian Associates Inc., Palo Alto, CA, USA) producing a homogeneous $\mathbf{B}_1$ field within the volume under investigation. The samples were located axially in the center of the coil and oriented with the cartilage surface perpendicular to the $\mathbf{B}_0$ field (the normal to the surface is parallel to the static field) to control for the magic angle effect. T_2 relaxation time mapping of the samples was conducted at 25 °C using a single spin echo sequence (TR = 2500 ms, TE = 14, 24, 34, 44, 64 and 84 ms, 1-mm slice thickness, 10-mm field-of-view, 256 × 64 matrix and six averages), with a 9.4 T Oxford 400 NMR vertical magnet (Oxford Instruments Plc., Witney, UK), a SMIS console (SMIS Ltd., Surrey, UK), equipped with 100 G/cm imaging gradients (45-mm bore). T_2 relaxation time maps were calculated by means of mono-exponential two-parameter fitting (MatLab 6.5.1, MathWorks Inc., Natick, MA, USA). For further analyses, depth-wise relaxation time profiles with a spatial resolution of 39 μm were determined from relaxation time maps by averaging 3-pixel-wide columns across the cartilage depth.

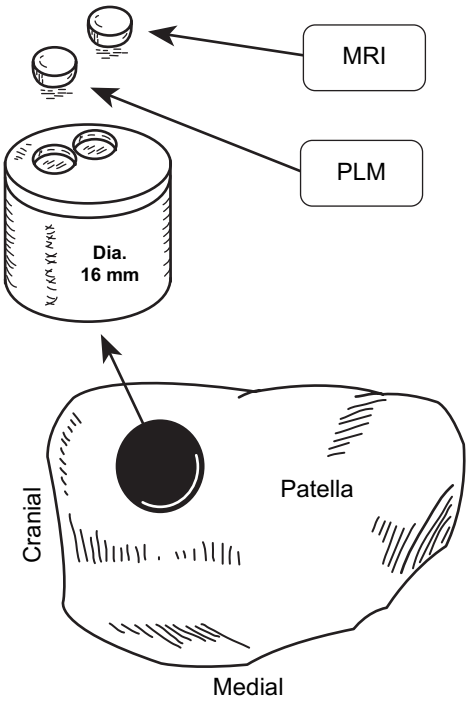

Fig. 1. Schematic drawing of the sampling location. A 16-mm osteochondral core was harvested from lateroproximal patella and subsequently, 4-mm cartilage discs were separated for MRI and PLM analyses.

POLARIZED LIGHT MICROSCOPY

Formalin-fixed non-stained paraffin-embedded samples were cut into three 5-μm-thick microscopical sections in two randomized orientations, as described previously[3,19]. For each sample, six sections were imaged and averaged. PLM measurements were conducted using a Leitz Ortholux BK-2 polarized light microscope (Leitz Messtechnik GmbH, Wetzlar, Germany) equipped with a cooled 12-bit CCD camera (Photometrics SenSys, Roper Scientific Inc., Tucson, AZ, USA), a monochromatic light source (wavelength 594 ± 3 nm), a pair of motor-controlled crossed polarizers[18] and a 6.3× strain free objective, yielding a spatial image resolution of 8.9 μm.

To determine collagen anisotropy and fibril angle, each section was imaged at multiple orientations of the crossed polarizers (0°, 15°, 30°, 45°, 60°, 75°, 90° and 90° with a λ/4-retardation plate)[18,20]. The degree of tissue anisotropy, i.e., index for parallelism of fibrils, was calculated as the ratio of intensity minimum and maximum, both taken from the least squares-fit of intensity vs rotation angle

curve[18]. In contrast to optical retardation or birefringence[21], anisotropy is a parameter that quantifies true parallelism of fibrils, not the general optical activity of fibrils[18]. Briefly, the anisotropy parameter demonstrates high values for highly organized tissue and low values for unorganized tissue. The fibril angle was determined from the orientation angle of the optical ellipse as calculated from the Stokes' parameters[20,22].

ANALYSIS OF THE LAMINAR STRUCTURE

PLM profiles were downsampled to match the spatial resolution of T_2 measurements. The relative thicknesses of histological zones, as determined from anisotropy profiles and T_2-laminae, were compared. For both PLM and MRI profiles, the depth of lamina/zone boundaries was determined for each rising and declining edge as the one-sided half-maximum value, a method adapted from Xia *et al.*[4]. For a typical tri-laminar T_2 profile, the first boundary is determined as the location of the left-side half-maximum value from the T_2 peak and the second boundary as the location of the right-side half-maximum value. A user assisted semi-automatic analysis program was made for this purpose in MatLab.

STATISTICAL ANALYSES

Linear correlation coefficients were calculated for T_2 and anisotropy profiles from each sample and for lamina/zone-thicknesses as determined from MRI and PLM. The Kruskal–Wallis *post hoc*-test was used for statistical comparison of relative lamina thicknesses, as determined either by T_2 or anisotropy measurements, between species for samples with identical laminar structure. The Bland–Altman plot[23] was used to assess the agreement of MRI and PLM techniques to determine the locations of lamina/zone boundaries.

Results

Based on the T_2 and anisotropy analyses, all human samples showed a typical tri-laminar appearance, while some porcine and bovine samples appeared to have five or seven laminae (Fig. 2, Table I). The spatial variation of T_2 was closely related to that of collagen fibril anisotropy and angle (Fig. 3). T_2 maxima were observed at fibril angles close to the magic angle. For human and bovine samples with three laminae, the angle profile showed an arcading structure, whereas porcine samples showed different behavior in deep tissue (Fig. 3). For samples with more than three T_2-laminae a complex variation of anisotropy and fibril angle was observed (Fig. 3). Anisotropy showed an inverse relationship with T_2: the mean correlation coefficients between T_2 and anisotropy profiles were $r = -0.79 \pm 0.11$, $r = -0.78 \pm 0.16$ and $r = -0.67 \pm 0.25$ for human, bovine and porcine specimens, respectively. After pooling the data from different species 44% ($r^2 = 0.44$, $P < 0.0001$) of the variations in T_2 appearance could be explained by the collagen anisotropy.

For samples with three laminae, human cartilage was significantly ($P < 0.05$) thicker (2.7 ± 0.6 mm) than bovine (1.5 ± 0.2 mm) or porcine (1.7 ± 0.2 mm) tissue, as determined by MRI. Similarly, significant difference in the absolute thicknesses was also observed by PLM (Table II). The relative (%) lamina thicknesses were not statistically different, a result consistent with PLM measurements (Table II). The samples measured by PLM were thicker than those measured by MRI ($P < 0.05$). For bovine and porcine samples with five laminae, a significant difference in the relative thicknesses of the laminae II and IV was

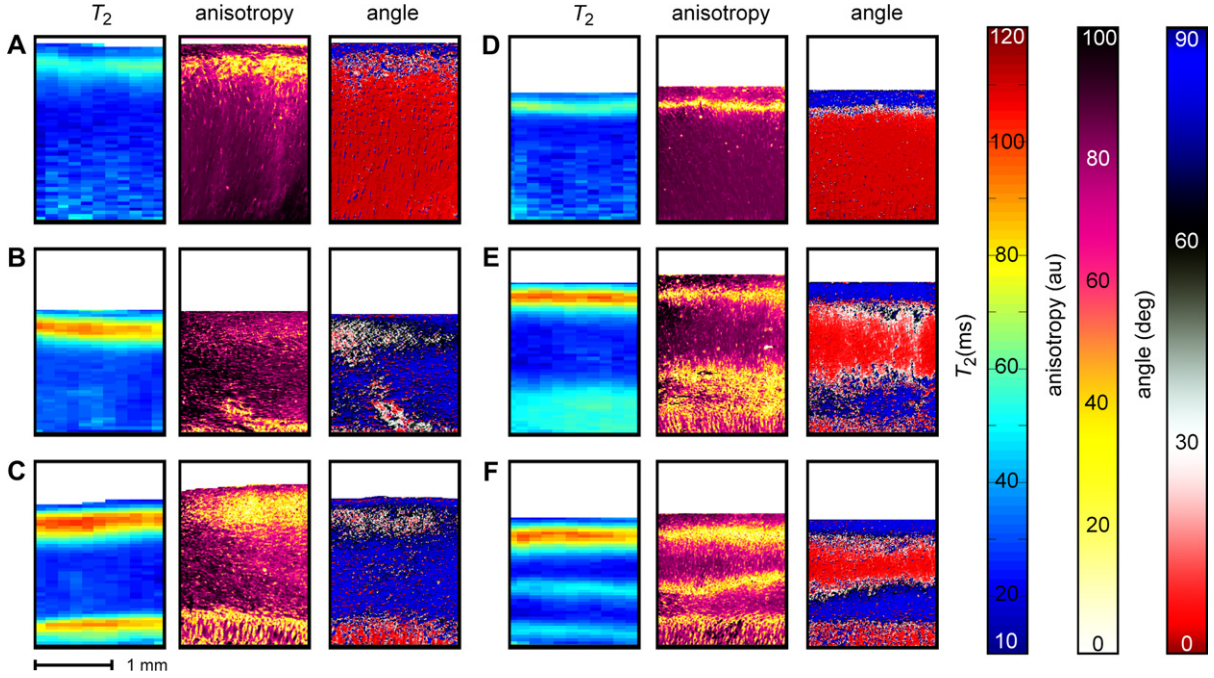

Fig. 2. Representative T_2, anisotropy and fibril angle maps for human cartilage showing three laminae (A), porcine cartilage showing three (B) or five (C) laminae, bovine cartilage showing three (D), five (E) or seven (F) laminae. The 1-mm scalebar shown down and left applies to all maps.

Table I
Number of tissue laminae as determined from T_2 relaxation time maps of human, bovine and porcine cartilage samples

Species	Age (years)	Number of samples with different laminae			Total number of samples
		3	5	7	
Human	22–78	12	0	0	12
Bovine	~1–3	8	3	1	12
Porcine	~0.3	7	4	0	11
Number of samples		27	7	1	35

observed: porcine samples showed a significantly thicker lamina II and bovine samples showed a thicker lamina IV, as determined by both techniques ($P < 0.05$, data not shown). The overall thickness of the samples between groups with five laminae was not statistically different.

Absolute thicknesses of individual laminae or zones (as assessed by MRI or PLM) were not statistically different. A high linear correlation between the zone thicknesses from MRI and PLM was revealed (correlation for all laminae were $r = 0.91$, $r = 0.95$ and $r = 0.91$ for human, bovine and porcine samples, respectively). Concomitantly, a statistically significant correlation was found between the zone locations determined from the different modalities [$r = 0.92$ for all species pooled, Fig. 4(A)]. The Bland–Altman plot revealed the agreement of the techniques in determining the depth of zone/lamina location in the present measurement geometry (Fig. 4).

Discussion

T_2 mapping and quantitative PLM, both known to be sensitive to the 3-D architecture of collagen network, were combined to show the potential of T_2 mapping in revealing collagen-associated features of healthy intact human, bovine and porcine cartilage, and to determine the extent to which collagen anisotropy, as measured by PLM, accounts for the depth-wise variation of T_2 relaxation time. The laminar/zonal appearance of collagen network varied between

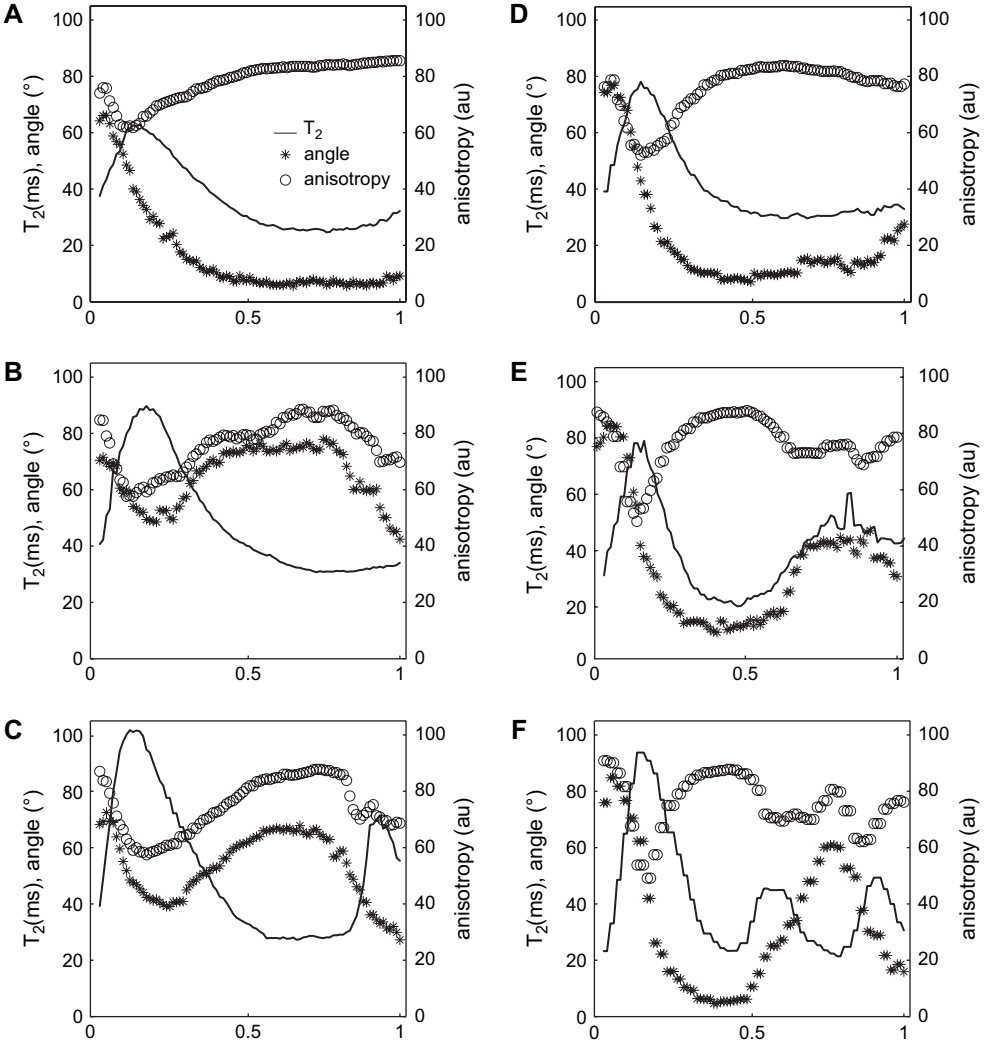

Fig. 3. Depth-normalized (from articular surface) mean profiles for T_2 and fibril angle and anisotropy as measured by PLM. Human samples showing three laminae (A), porcine samples showing three (B) or five (C) laminae, bovine samples showing three (D), five (E) or seven (F) laminae. In all figures, solid line denotes T_2, star (*) denotes fibril angle and circle (○) denotes anisotropy.

Table II
Mean relative thickness ± SD of the cartilage laminae, as observed in different species by T_2 (d_{T_2}) and anisotropy ($d_{Anisotropy}$) (PLM) analyses. Only data from the samples with three laminae are included

Lamina/zone	Human ($n=12$)		Bovine ($n=8$)		Porcine ($n=7$)	
	d_{T_2} (%)	$d_{\text{Anisotropy}}$ (%)	d_{T_2} (%)	$d_{\text{Anisotropy}}$ (%)	d_{T_2} (%)	$d_{\text{Anisotropy}}$ (%)
I	5.5 ± 2.4	5.2 ± 2.2	5.6 ± 1.9	7.3 ± 3.3	5.1 ± 2.4	5.5 ± 2.7
II	24.0 ± 10.8	19.5 ± 10.1	18.3 ± 7.3	14.3 ± 4.3	28.2 ± 9.9	23.2 ± 9.0
III	70.5 ± 12.2	75.4 ± 11.4	76.1 ± 8.3	78.5 ± 6.4	66.7 ± 9.3	71.4 ± 10.2
Total thickness (mm)	2.7 ± 0.6	3.3 ± 0.8	1.5 ± 0.2**	1.7 ± 0.3**	1.7 ± 0.2*	1.9 ± 0.3**

Statistically different as compared to human (*$P < 0.05$, **$P < 0.01$) (Kruskal–Wallis *post hoc*-test).

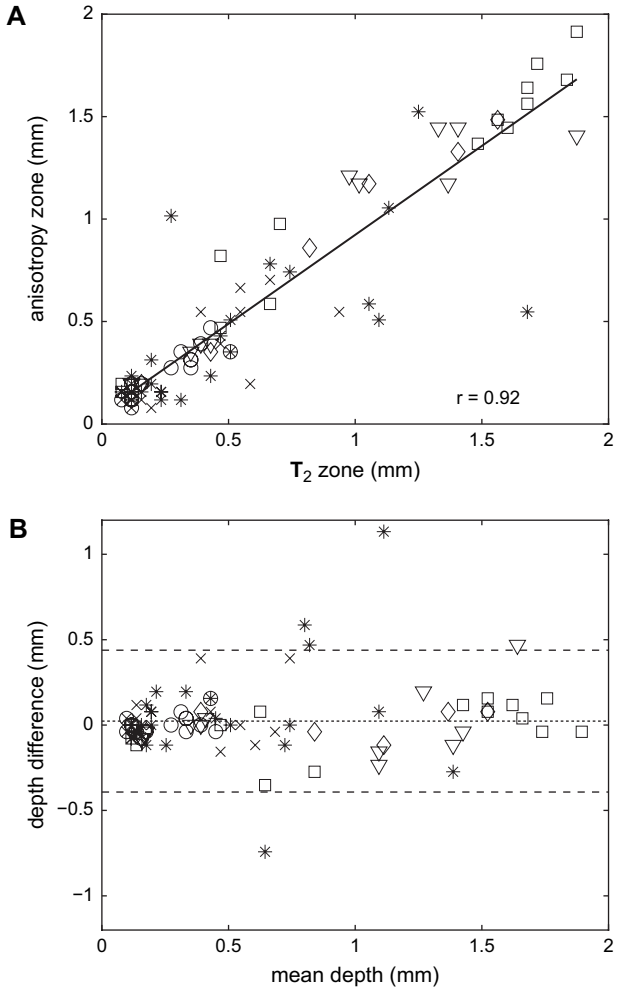

Fig. 4. Linear correlation (A) and Bland–Altman plots (B) for laminar boundary locations as determined by T_2 and anisotropy profiles. The plot shows a mean difference of 0.02 mm (less than the spatial resolution) for the laminar boundary locations, as detected by T_2 and PLM. Star (*) denotes human samples, circle (○) bovine with three laminae, triangle (▽) bovine with five laminae, diamond (◇) bovine with seven laminae, cross (×) porcine with three laminae and square (□) porcine samples with five laminae. Dotted line indicates the mean of the difference and dashed lines ±2SD. The two measurements with large (>0.7 mm) differences in boundary locations (outlier points) were from samples with variable focal degeneration within the tissue under examination, resulting in inaccurate determination of the zone boundaries.

species and was similarly observed using both MRI and PLM techniques. The structure of mature human cartilage was consistent with the classical Benninghoff model that describes three distinct collagenous zones, while juvenile animal tissue showed three, five or seven laminae or zones[24]. The thicknesses of different collagenous zones, as derived from both MRI and PLM measurements, were in good agreement, as also seen in several previous studies[3–5,14].

Previous studies relating T_2 relaxation time or T_2-weighted signal to PLM have shown the close association between T_2-laminae and the collagen network[4,5,7,11,13,15,25]. The quantitative derivation of the fibril angle from PLM data has provided further evidence for the angular dependence of T_2[4,15]. In this study, the angle profiles for human and bovine cartilage with three laminae were qualitatively consistent with the arcading collagen structure and followed the changes in T_2. Porcine samples as well as the extra-laminated bovine samples appeared different in the deep tissue, showing significantly higher fibril angle values. This difference is likely related to incomplete maturation of the collagenous network, an issue requiring further investigation. The angle values at which the T_2 maxima appeared were roughly equal in each group and at each maximum, though the values were not exactly the magic angle. It should be noted that the anisotropy and fibril angle are inter-connected and require simultaneous consideration. In tissue with low anisotropy the fibril orientation determines only the average course of the fibrils in the region of interest. Anisotropy provides a measure that defines how parallel the fibrils are aligned, i.e., the anisotropy is the ''standard deviation'' of the measured fibril orientation.

The connection between T_2 and optical birefringence[3] and the close agreement between thicknesses of T_2-laminae and histological zones as determined from PLM angle profiles have been shown earlier[4,15]. The present study is the first one to relate T_2 with the PLM-measured collagen anisotropy, a quantitative, physical measure of the preferential arrangement of fibrils[18]. In contrast to optical retardation or birefringence, anisotropy is a true measure of fibril parallelism[18]. The depth-wise variation of T_2 was highly correlated with collagen anisotropy and was clearly dependent on the fibril angle. Consequently, the zonal thicknesses determined from T_2 and anisotropy profiles were in good agreement. According to our results 60% of the depth-wise variation of T_2 in human (and 44% with pooled data from all species) is accounted for by the changes in collagen anisotropy. The remainder is contributed to by the orientation-independent relaxation mechanisms, influenced by the content and mobility of water and macromolecular concentration of tissue, as well as by uncertainties in experimental measurements, such as sample preparation. In the present study, local

tissue PG content was not related to T_2 analyses. Earlier, the influence of altered mobility of water after enzymatical PG depletion had no significant effect on T_2, suggesting that T_2 is mainly dependent on the collagen fibril network structure[11]. Although Wayne *et al.* observed a T_2 increase after PG-cleavage with chondroitinase[12], the present significant connection between the collagen orientation and T_2 relaxation time is undisputable.

The cartilage samples showed three, five or seven T_2-laminae. PLM confirmed that these features were associated with actual histological zones. Additional laminae have previously been observed by us[3] and others[5,15]. Our quantitative PLM results suggest that significant remodelation of the collagen network takes place during the maturation process[16]. A study on pediatric cartilage showed similar spatial variation of patellar T_2 profiles between children of mean ages 8.2 and 14.2 years, but an overall decrease in the T_2 values of older children was observed[26]. Similar trilaminar structure was seen in the human samples of the present study. Furthermore, changes occurring in mature, aging human tissue have also been reported to have an impact on T_2[27]. Structural and compositional changes have been shown to occur in porcine cartilage during 3 days to 30 weeks of age[28]. Significant decrease in T_2 relaxation time during maturation has been reported earlier in rat patella[29,30], with no significant variations during aging process after maturation[29]. Olivier also demonstrated structural differences in T_2 of maturing cartilage, i.e., complex laminar structure was seen in calf cartilage whereas more mature tissue exhibited a simpler network pattern.[31] The number of the laminae may also be related to the sampling location in the joint (load-bearing vs non-bearing), as was demonstrated earlier in canine humeral head[15]. In the present study, the anatomical location was identical for all samples. Given the varying age of the different species in the present study (young and adult bovine, young porcine and adult human) the additional laminae in deeper cartilage, as well as the inter-species differences, likely relate to the varying stages of tissue maturation.

While T_2 reliably provided information on the collagen architecture, some limitations prevail in the present study. First, microscopic sections were prepared from the osteochondral blocks whereas samples for MRI were detached from the underlying bone. This may have subjected samples to different amounts of inhomogeneous swelling resulting in possible inaccuracies of profile matching and an occasional minor increase in the deepmost T_2 values. The removal of the subchondral bone may thus influence the deepmost T_2 values by facilitating saline diffusion into the cartilage. A recent study, however, showed that the orientation of collagen fibrils in deep tissue remains unchanged after detaching from bone, while the density of the collagen fibrils may change[32]. Second, when detaching the MRI samples from the bone some cartilage may be left attached to the bone, resulting in an error in the thickness of the deepest lamina. This also resulted in the systematic difference of MRI-derived cartilage thickness being less than that determined from microscopy. Yet, the number of laminae observed by PLM measurements agreed to that of MRI analyses and therefore this error is probably not very significant. Third, as discussed in our previous studies[3] and by Xia *et al.*[33], MRI provides a measure of a 3-D volume, whereas PLM is a two-dimensional measurement, although this is attempted to compensate for by imaging sections cut in several directions. Fourth, and probably most importantly, PLM analyses were made from tissue adjacent to the MRI samples, and therefore are not exactly from the same anatomical location (Fig. 1). This may result in the comparison of slightly different tissue. We have observed that changes in the collagen architecture may be highly local and morphology can vary within a small distance. These limitations are likely to explain the occasional incoherence observed between the T_2 and PLM profiles. Additionally, the freeze-thaw cycle might affect the cartilage T_2 values, however, earlier studies have shown that T_2 values of thawed tissue are identical to those of fresh cartilage[30].

This study extends our previous efforts to systematically validate and interpret T_2 relaxation of cartilage[3,11]. The present results show that, regardless of the species and maturation, T_2 relaxation time can serve as an indirect quantitative parameter to describe the structural properties of the collagen network of healthy articular cartilage, and provide indirect morphological information on the structure. *In vivo* T_2 mapping is clinically feasible[6] and it could potentially be used for both assessing the maturation of cartilage and the evaluation of cartilage repair. The effect of maturation on cartilage T_2 should also be considered when studying cartilage disorders. Furthermore, the significant structural variation of healthy juvenile cartilage, as seen in this study, should be carefully recognized since animal tissue is widely used as a model for mature human cartilage.

Acknowledgments

Juhana Hakumäki, M.D., Ph.D. and Johanna Närväinen, Ph.D. are gratefully acknowledged for technical assistance in MRI measurements. Financial support from the Finnish Graduate School in Skeletal Diseases, Ministry of Education in Finland; Instrumentarium Science Foundation; the Finnish Cultural Foundation of Northern Savo; the National Technology Agency (TEKES, projects 40714/01 and 70037/01), Finland; the Academy of Finland (grant 205886); Kuopio University Hospital (EVO, project 5031329), Kuopio, Finland and Sigrid Juselius Foundation is acknowledged.

References

1. Buckwalter JA, Mankin HJ. Articular cartilage, part II: degeneration and osteoarthrosis, repair, regeneration, and transplantation. J Bone Joint Surg Am 1997;79(4): 612–32.
2. Mow VC, Zhu W, Ratcliffe A. Structure and function of articular cartilage and meniscus. In: Mow VC, Hayes WC, Eds. Basic Orthopaedic Biomechanics. New York: Raven Press, Ltd 1991:143–198.
3. Nieminen MT, Rieppo J, Töyräs J, Hakumäki JM, Silvennoinen MJ, Hyttinen MM, *et al.* T2 relaxation reveals spatial collagen architecture in articular cartilage: a comparative quantitative MRI and polarized light microscopic study. Magn Reson Med 2001; 46(3):487–93.
4. Xia Y, Moody JB, Burton-Wurster N, Lust G. Quantitative *in situ* correlation between microscopic MRI and polarized light microscopy studies of articular cartilage. Osteoarthritis Cartilage 2001;9(5):393–406.
5. Grunder W, Wagner M, Werner A. MR-microscopic visualization of anisotropic internal cartilage structures using the magic angle technique. Magn Reson Med 1998;39(3):376–82.

6. Mosher TJ, Dardzinski BJ. Cartilage MRI T2 relaxation time mapping: overview and applications. Semin Musculoskelet Radiol 2004;8(4):355–68.
7. Menezes NM, Gray ML, Hartke JR, Burstein D. T2 and T1rho MRI in articular cartilage systems. Magn Reson Med 2004;51(3):503–9.
8. Fragonas E, Mlynarik V, Jellus V, Micali F, Piras A, Toffanin R, *et al*. Correlation between biochemical composition and magnetic resonance appearance of articular cartilage. Osteoarthritis Cartilage 1998;6(1): 24–32.
9. Lusse S, Claassen H, Gehrke T, Hassenpflug J, Schunke M, Heller M, *et al*. Evaluation of water content by spatially resolved transverse relaxation times of human articular cartilage. Magn Reson Imaging 2000;18(4):423–30.
10. Shapiro EM, Borthakur A, Kaufman JH, Leigh JS, Reddy R. Water distribution patterns inside bovine articular cartilage as visualized by 1H magnetic resonance imaging. Osteoarthritis Cartilage 2001;9(6): 533–8.
11. Nieminen MT, Töyräs J, Rieppo J, Hakumäki JM, Silvennoinen J, Helminen HJ, *et al*. Quantitative MR microscopy of enzymatically degraded articular cartilage. Magn Reson Med 2000;43(5):676–81.
12. Wayne JS, Kraft KA, Shields KJ, Yin C, Owen JR, Disler DG. MR imaging of normal and matrix-depleted cartilage: correlation with biomechanical function and biochemical composition. Radiology 2003;228:493–9.
13. Goodwin DW, Dunn JF. High-resolution magnetic resonance imaging of articular cartilage: correlation with histology and pathology. Top Magn Reson Imaging 1998;9(6):337–47.
14. Grunder W, Kanowski M, Wagner M, Werner A. Visualization of pressure distribution within loaded joint cartilage by application of angle-sensitive NMR microscopy. Magn Reson Med 2000;43(6):884–91.
15. Xia Y, Moody JB, Alhadlaq H, Hu J. Imaging the physical and morphological properties of a multi-zone young articular cartilage at microscopic resolution. J Magn Reson Imaging 2003;17(3):365–74.
16. Rieppo J, Hyttinen MM, Halmesmäki E, Ruotsalainen H, Vasara A, Kiviranta I, *et al*. Remodelation of collagen network architecture during cartilage maturation. Trans Orthop Res Soc 2004;29:549.
17. Rieppo J, Halmesmäki EP, Siitonen U, Laasanen MS, Töyräs J, Kiviranta I, *et al*. Histological differences in human, bovine and porcine cartilage. Trans Orthop Res Soc 2003;28:589.
18. Rieppo J, Hallikainen J, Jurvelin JS, Helminen HJ, Hyttinen MM. Novel quantitative polarization microscopic assessment of cartilage and bone collagen birefringence, orientation and anisotropy. Trans Orthop Res Soc 2003;28:570.
19. Király K, Hyttinen MM, Lapveteläinen T, Elo M, Kiviranta I, Dobai J, *et al*. Specimen preparation and quantification of collagen birefringence in unstained sections of articular cartilage using image analysis and polarizing light microscopy. Histochem J 1997; 29(4):317–27.
20. Collett E. Polarized Light: Fundamentals and ApplicationsIn: Optical Engineering Series. New York: Mercel Dekker 1992, 91–122.
21. Arokoski JP, Hyttinen MM, Lapveteläinen T, Takacs P, Kosztaczky B, Modis L, *et al*. Decreased birefringence of the superficial zone collagen network in the canine knee (stifle) articular cartilage after long distance running training, detected by quantitative polarised light microscopy. Ann Rheum Dis 1996;55(4): 253–64.
22. Bennett HS. Methods applicable to the study of both fresh and fixed materials. The microscopical investigation of biological materials with polarized light. In: McClung JR, Ed. McClung's Handbook of Microscopical Technique. New York: Paul B Hoeber 1950: 591–677.
23. Bland JM, Altman DG. Statistical methods for assessing agreement between two methods of clinical measurement. Lancet 1986;1(8476):307–10.
24. Benninghoff A. Form und Bau der Gelenkknorpel in ihren Beziehungen zur Function. Erste Mitteilung: die modellierenden und formerhaltenden Faktoren des Knorpelreliefs. Z Anat 1925;76:43–63.
25. Rubenstein JD, Kim JK, Morova-Protzner I, Stanchev PL, Henkelman RM. Effects of collagen orientation on MR imaging characteristics of bovine articular cartilage. Radiology 1993;188(1):219–26.
26. Dardzinski BJ, Laor T, Schmithorst VJ, Klosterman L, Graham TB. Mapping T2 relaxation time in the pediatric knee: feasibility with a clinical 1.5-T MR imaging system. Radiology 2002;225(1):233–9.
27. Mosher TJ, Liu Y, Yang QX, Yao J, Smith R, Dardzinski BJ, *et al*. Age dependency of cartilage magnetic resonance imaging T2 relaxation times in asymptomatic women. Arthritis Rheum 2004;50(9): 2820–8.
28. Nakano T, Aherne FX, Thompson JR. Changes in swine knee articular cartilage during growth. Can J Anim Sci 1978;59:167–79.
29. Watrin A, Ruaud JP, Olivier PT, Guingamp NC, Gonord PD, Netter PA, *et al*. T2 mapping of rat patellar cartilage. Radiology 2001;219(2):395–402.
30. Watrin-Pinzano A, Ruaud JP, Olivier P, Grossin L, Gonord P, Blum A, *et al*. Effect of proteoglycan depletion on T2 mapping in rat patellar cartilage. Radiology 2005;234(1):162–70.
31. Olivier P, Loeuille D, Watrin A, Walter F, Etienne S, Netter P, *et al*. Structural evaluation of articular cartilage: potential contribution of magnetic resonance techniques used in clinical practice. Arthritis Rheum 2001;44(10):2285–95.
32. Keinan-Adamsky K, Shinar H, Navon G. The effect of detachment of the articular cartilage from its calcified zone on the cartilage microstructure, assessed by (2)H-spectroscopic double quantum filtered MRI. J Orthop Res 2005;23(1):109–17.
33. Xia Y, Moody JB, Alhadlaq H. Orientational dependence of T2 relaxation in articular cartilage: a microscopic MRI (microMRI) study. Magn Reson Med 2002;48(3):460–9.